P2-2

Analysis of the Leakage Mechanism of Sub-110nm DRAM Shallow Junctions with Titanium and Cobalt Silicided Contacts after Heat Budget

S.B. Kang, H.S. Park, K.J. Moon, S.G. Yang, G.H. Choi, U.I. Chung and J.T. Moon

Process and Development Team, Semiconductor R&D Center, Samsung Electronics Co. Ltd.,
San #24, Nongseo-Ri, Kiheung-Eup, Yongin-City, Kyungki-Do, KOREA 449-711
Phone : 82-31-209-3663, Fax : 82-31-209-6299, E-mail : sbkangh@samsung.co.kr

1. Abstract

The junction leakage mechanisms of n+/p and p+/n shallow junctions with $TiSi_2$ and $CoSi_2$ contacts are analyzed. Nearly pure generation currents caused by the phonon-assisted tunneling are observed in all cases with the exception of p+/n $TiSi_2$ at low electric field in which the Pool-Frenkel barrier lowering effect was responsible for the reverse leakage current.

2. Introduction

Suppressing the leakage current in metallized source and drain contacts has been a key requirement in DRAM in addition to achieving a low contact resistance. However, the post heat budget in COB (Capacitor Over Bit-Line) structured DRAM results in a high contact resistance, especially in metal/p+ contacts, when titanium silicide is employed. A promising alternative for titanium silicided contact is cobalt silicided contact. The present investigation reports the analysis and comparison of the leakage mechanism in shallow junctions with titanium and cobalt silicided contacts after high heat budget associated with the capacitor process.

3. Experiments

A 110nm CMOS technology was used to fabricate n+/p and p+/n shallow junctions with multiple titanium and cobalt silicided contacts. The depths of the junction and shallow trench isolation (STI) were 110nm and 250nm, respectively. The size of the silicide contact was 130nm. Titanium silicide was formed in contacts by depositing PECVD-Ti. Cobalt silicide was formed by 2 step anneal salicide process. During the capacitor integration, 750℃ 60min thermal budget was applied to observe its effect on the junction leakage.

4. Results and Discussion

Fig.1 shows the forward and reverse bias I-V characteristics of the n+/p and p+/n junctions with titanium and cobalt silicided contacts measured at various temperatures. A gradual increase of the reverse leakage currents with measuring temperature is observed in $TiSi_2$ contaced junctions while an abrupt increase is observed in $CoSi_2$ contaced junctions.

Arrhenius plot of the reverse current (log I/T^3 vs. 1/T) of each diode at reverse voltage of 3.5V indicates that the activation energies of all diodes are either near or below the half of the Si energy gap as shown in Fig.2. The results in Fig.2 show that the reverse leakage currents of both $TiSi_2$ and $CoSi_2$ contacted junctions are generation-recombination currents instead of diffusion currents.

The portions of diffusion and generation-recombination currents of each diode are separated by I vs. 1/C plot in Fig.3 as proposed by Murakami et al. [1,2] By extrapolating the leakage current to 1/C=0 where generation current is absent, the current components can be separated. Table I illustrates the result of the component separation at reverse voltage of 3.5V measured at 25C.

The results indicate that the generation-recombination component of the leakage current dominates in all cases.

The mechanisms responsible for the generation currents in each case are further analyzed by the method proposed by Theunissen et al in which the mechanism for the electric field dependant generation current can be identified as either Pool-Frenkel barrier lowering or phonon-assisted tunneling. [3] Fig. 4 shows the Arrhenius plots of log I vs. 1/T of n+/p and p+/n diodes with $TiSi_2$ and $CoSi_2$ contacts. The activation energies from the slopes in Fig.4 are plotted as a function of the reverse voltage in Fig.5. By combining Fig.5 with the relationship between the electric field (F) and the reverse voltage as shown in Fig.6, the activation energies are plotted as a function of the square root of the electric field in Fig.7. The results in Fig.7 show that only the p+/n diode with TiSi2 contact at low electric field exhibits the Pool-Frenkel barrier lowering since the slope of Ea vs. $F^{1/2}$ in Pool-Frenkel barrier lowering is supposed to be linear. The value of the ionization energy of the emission center with n+/p $TiSi_2$, which is calculated from the extrapolation of the Ea at zero field, is about 0.7eV which is in good agreement with the previously reported values. [3] The rest of the diodes such as n+/p $TiSi_2$, n+/p $CoSi_2$ and p+/n $CoSi_2$ exhibit a domination of an additional barrier lowering effect such as phonon-assisted tunneling.

The result of Fig.7 is reconfirmed by the fitting the I-V characteristics of each diode to theoretical Pool-Frenkel emission plot of I/V vs. $V^{1/2}$ as shown in Fig.8. The only case in which a characteristic linearity is observed is p+/n diode with $TiSi_2$ contact, which is in good agreement with the Ea vs. $F^{1/2}$ plot.

The difference in the mechanism of the generation current in p+/n diodes with $TiSi_2$ and $CoSi_2$ contact can be explained by the effect of the silicide-induced generation of phonon-assisted tunneling with $CoSi_2$ contact. The VSEM images of $TiSi_2$ and $CoSi_2$ contacts in Fig.9 indicate that the protrusion and the magnitude of diffusion of cobalt in both the lateral and longitudinal direction exceeds that of titanium.

5. Conclusions

The reverse leakage characteristics of n+/p and p+/n diodes with $TiSi_2$ and $CoSi_2$ contacts were compared and analyzed in sub-110nm DRAM shallow junctions. All diodes exhibited a nearly pure generation current probably due to the formation of high density traps induced by implantation damages. With the exception of p+/n $TiSi_2$ at low electric field, the dominant mechanism of the generation current was the phonon-assisted tunneling. The Pool-Frenkel barrier lowering effect was observed only in p+/n $TiSi_2$ diode. The difference in the current mechanism in p+/n diodes with $TiSi_2$ and $CoSi_2$ contacts can be explained by the excessive diffusion of cobalt into the shallow junction after high thermal budget post-treatment.

References

[1] Y.Murakami and T.Shingyouji, J.Appl.Phys. 75(7), 1994, p3548.
[2] H.Uchiyama, K.Matsumoto, T.Mchedlidze, M.Nisimura and K.Yamabe, J.Electrochem.Soc. 146(6), 1999, p2322.
[3] M.J.J.Theunissen and F.J.List, Solid-State Electronics 28(5), 1985, p417.

Table I. Current component separation (3.5V, 25℃)

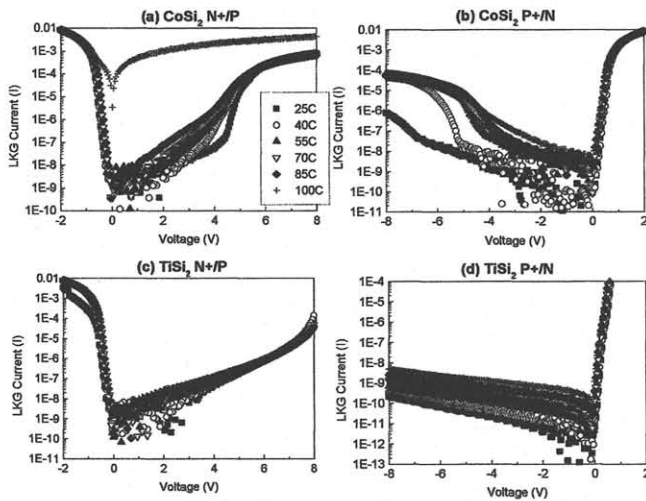|	$TiSi_2$ n+/p	$TiSi_2$ p+/n	$CoSi_2$ n+/p	$CoSi_2$ p+/n
I total	2.97e-08A	2.68e-08A	2.72e-09A	1.86e-11A
I diffusion	2.00e-13A	5.00e-14A	3.00e-15A	1.00e-14A
I generation	2.97e-08A	2.68e-08A	2.72e-09A	1.86e-11A

Fig.1 Forward and reverse bias I-V characteristics of the n+/p and p+/n junctions with titanium and cobalt silicide contacts measured at various temperatures
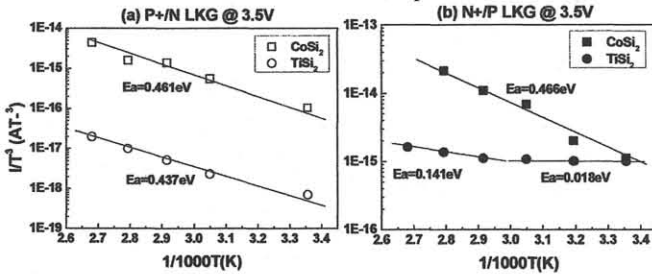

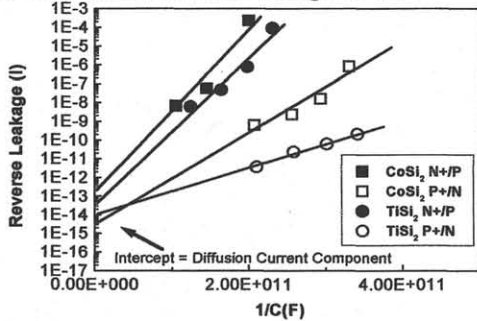Fig.2 Arrhenius plots of the reverse current (log I/T^3 vs. $1/T$) of each diode at reverse voltage of 3.5V

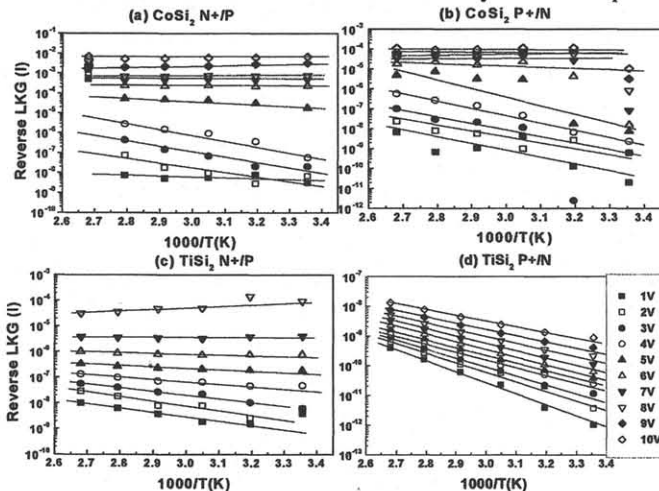Fig.3 Component separation of diffusion and generation-recombination currents of each diode by I vs. 1/C plot.

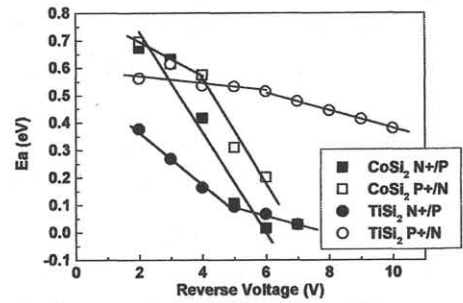Fig.4 Arrhenius plots of log I vs. 1/T of n+/p and p+/n diodes with TiSi$_2$ and CoSi$_2$ contacts.

Fig.5 Activation energies as a function of the reverse voltages
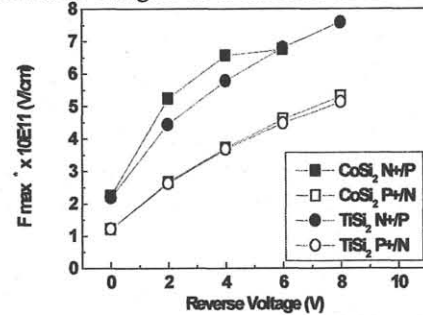

Fig.6 The relationship between electric field and the reverse V.
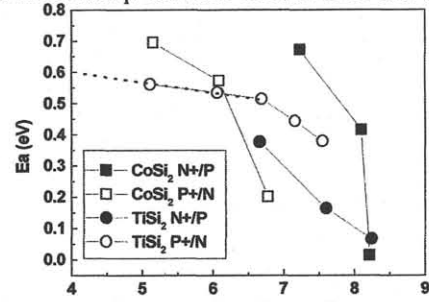

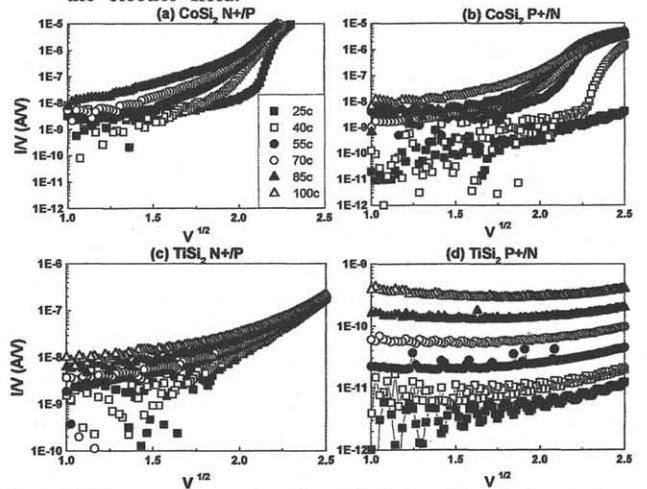Fig.7 Activation energies as a function of the square root of the electric field.

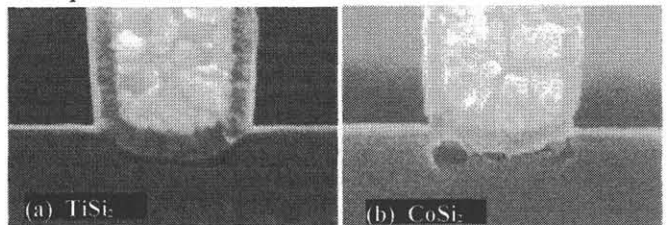Fig.8 Fitting results to the theoretical Pool-Frenkel emission plot of I/V vs. $V^{1/2}$.

Fig.9 VSEM images of TiSi$_2$ and CoSi$_2$ contacs